

# Lifetime measurements of the $4f^{14}5d$ metastable states in single ytterbium ions

N. Yu and L. Maleki

Jet Propulsion Laboratory, California Institute of Technology, 4800 Oak Grove Drive, Pasadena, California 91109

(Received 26 July 1999; published 12 January 2000)

The ytterbium ion has a rich level structure of low-lying states, and is one of the most widely used in experiments with trapped ions. We have measured the radiative lifetimes for the two  $4f^{14}5d$  metastable states using single ytterbium ions confined in a rf trap. The obtained lifetimes for  $D_{3/2}$  and  $D_{5/2}$  states are 52.7(2.4) and 7.0(0.4) ms, respectively. The results are in good agreement with previously measured values, but differ significantly from theoretical estimates. The  $P_{1/2}$  branching ratio into  $D_{3/2}$  has also been obtained from the experiment to be 0.0483 with a 9% uncertainty.

PACS number(s): 32.70.Cs, 32.80.Pj, 42.50.Lc

## I. INTRODUCTION

The ytterbium ion is considered as the most versatile atomic species used in trapped-ion frequency standards and atomic clocks. The low-lying energy level of this ion has a very rich structure, and is suitable as a basis for microwave, infrared, or optical frequency references [1–6]. For the same reason, the  $\text{Yb}^+$  ion is also well suited for other possible applications such as cavity QED studies and the demonstration of quantum computation using trapped ions.

The energy-level scheme of the low-lying states of  $\text{Yb}^+$  ion is shown in Fig. 1. The  $D_{5/2}$  state decays to the ground state via a weak electric quadrupole transition at 411 nm. This level is of particular interest as the basis for an optical frequency standard. On the other hand, the metastable  $D_{3/2}$  state, like that in other alkalinelike ions, is often more of an experimental nuisance. This is because the laser at the  $S_{1/2}$ - $P_{1/2}$  transition required to cool the ion optically pumps the ion into this level, and so a clearing laser is necessary to depopulate it. Nevertheless the existence of the  $D_{3/2}$  state makes it possible to design the cooling transition and achieve a lower-temperature limit [8]. Moreover, the  $D_{3/2}$  state in  $\text{Yb}^+$  has transitions to several upper mixed states with transition widths in the MHz range, which may be well suited for cavity QED studies [9]. It is thus clear that an accurate knowledge of the lifetimes of these two levels is quite important for many applications. The radiative lifetime for the  $D_{5/2}$  of  $\text{Yb}^+$  has been measured previously with single trapped ions. It was found to be  $7.2 \pm 0.3$  ms, which corresponds to a natural linewidth of 22 Hz [7]. This value is in significant disagreement with the theoretical calculations. The radiative lifetime of the  $D_{3/2}$  state of  $\text{Yb}^+$  has also been measured before, but with ion clouds in buffer gases [10]. However, it has been shown that measurements using ion clouds in a buffer gas could lead to considerable errors, particularly for long-lived states [11]. Since the value obtained with this technique is also in disagreement with the theoretical calculations, ideally a singly confined ion in ultrahigh vacuum should be used to measure this lifetime to eliminate all possible collisional effects.

This paper presents lifetime measurements on both metastable  $D$  states in  $\text{Yb}^+$  using single trapped ions. Section II gives a brief description of the experimental setup. Sections

III and IV describe the measurements for the  $D_{3/2}$  and  $D_{5/2}$  states, respectively. While the measurement for  $D_{5/2}$  in this work is similar to previous measurements using the quantum jump technique, the lifetime measurement of the  $D_{3/2}$  state in  $\text{Yb}^+$  was carried out with individual ions for the first time to our knowledge using a new measurement technique.

## II. EXPERIMENT

A sketch of the experimental setup is shown in Fig. 2. A small Paul-Straubel trap [12] was used to confine single  $\text{Yb}^+$  ions. The trap is a 1-mm-diameter wire loop made with 125- $\mu\text{m}$ -diameter tantalum wire twisted at two sides as support leads. It was driven by a 11-MHz rf source. Typical applied rf voltages were about 700 V, producing about 1-MHz axial secular frequency. Because of stray dc fields, an enhanced micromotion of the trapped ions was present. To reduce this micromotion, an externally applied compensation was used. However, only one compensation electrode was used, roughly along the direction of the cooling laser, since the micromotion perpendicular to the laser beam could not be detected in the present setup.

Ytterbium ions were produced near the trap by directing ytterbium atoms emanating from an oven, and the ionizing

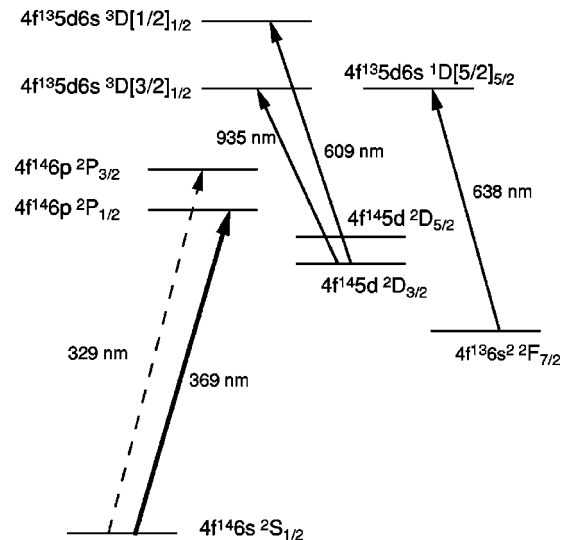


FIG. 1.  $\text{Yb}^+$  energy-level scheme of the low-lying states (not to scale).

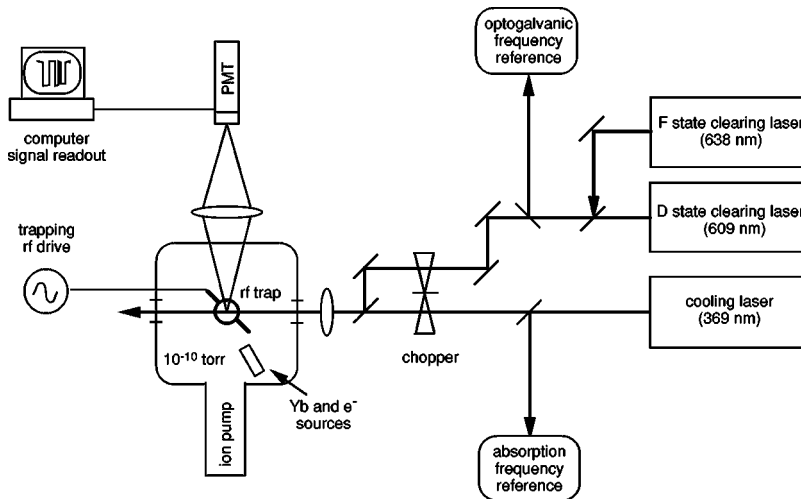


FIG. 2. Block diagram of the experimental setup.

electrons, toward the trap. The ytterbium used in the source had a natural isotopic abundance, but only the  $^{174}\text{Yb}^+$  isotope was selectively loaded. The selection was achieved by appropriately detuning the 369-nm cooling uv radiation which was generated from a frequency-doubled Ti:sapphire laser. As mentioned in Sec. I, the presence of the lower-lying  $D_{3/2}$  state required the use of a clearing laser to achieve continuous fluorescence. This can be either a 609-nm laser or a 935-nm laser. For the work presented in this paper, a 609-nm dye laser was used. The transition excited by this laser has a linewidth of about 4 MHz; the micromotion sidebands at 11 MHz can therefore be readily resolved. We used the 609 spectrum as a convenient monitor for the micromotion reduction [13]. Both laser outputs at 369 and 609 nm were referenced to the absorption lines in  $\text{Yb}^+$  discharge lamps. The 369-nm line used the direct absorption with a homemade see-through discharge lamp, while the 609-nm absorption was detected using the optogalvanic spectroscopy technique.

The fluorescence photons were collected through an imaging lens and focused into a 50- $\mu\text{m}$  pinhole right in front of a solar-blind photomultiplier tube (PMT). A 50% transmitting bandpass filter centered at 369 nm was used to cut down the background light. With a single cooled  $\text{Yb}^+$  ion, up to  $1.6 \times 10^4$  photons were counted against less than 100 counts of background. As we will see in the following sections, the large signal-to-background ratio is crucial for reliable quantum jump detection on the millisecond scale.

### III. MEASUREMENT OF $D_{3/2}$ LIFETIME

The lifetime of  $D_{3/2}$  in the  $\text{Yb}^+$  ion has been measured previously with ion clouds in buffer gas [10]. It is not obvious how the measurement can be made with a single ion because the state is inside the transition cycle of the normal signal detection. Thus a variation of the quantum jump technique was used previously for measuring the  $D_{3/2}$  state in  $\text{Ba}^+$  [11]. This method cannot be conveniently adapted for the  $\text{Yb}^+$  measurement because of the much shorter lifetimes of the  $D$  states of  $\text{Yb}^+$ . Measurement of this lifetime with a single ion requires that a technique be developed.

Our measurement method takes advantage of the fact that

the branching ratio of  $P_{1/2}$  decaying to the ground state is large, about 200. In other words, an ion will emit an average of 200 uv photons before being pumped into the  $D_{3/2}$  state again. If one uses a very short 369-nm pulse, much shorter than the  $D_{3/2}$  state lifetime, then a detection of the 200 fluorescence photons would signal that the ion has decayed to the ground state. A short pulse is also necessary to achieve a large enough signal-to-background ratio, since the useful signal photons are emitted in the first few microseconds. In reality, the photon detection efficiency was rather low, about 0.03%. Thus state detection with a single pulse would be hopelessly insufficient. Fortunately, one is only interested in the probability in the lifetime measurement and, therefore, can accumulate the photon counts at a fixed wait time  $t_w$  over many repetitions. The total accumulated fluorescence count should be proportional to the probability of the ion having decayed within the wait time, i.e.,  $(1 - e^{-t_w/\tau})$ .

The measurement sequence started with a short cooling period with both the cooling and clearing lasers on. Then both lasers were turned off with the clearing laser off-time trailing that of the cooling laser. The ion was then left in the ground state. Subsequently, the uv laser was pulsed for a short time to pump the ion into the  $D_{3/2}$  state for the free decay. Photons scattered in this pulse period serve as the  $t = 0$  signal. After a given time  $t_w$ , another short uv pulse was switched on for the state detection. Finally, both lasers were turned on again and the measurement process was repeated. This laser pulse sequence is illustrated in Fig. 3. At the same time, the photon signal of the PMT was sent to a multichannel scaler (MCS). The MCS was triggered at a fixed point in the laser-cooling period with a fixed bin width of 10.24  $\mu\text{s}$ . The top trace of Fig. 3 are sample data collected on the MCS. Peak *A* is the ion fluorescence at the cooling period, peak *B* is the  $t = 0$  signal, and peak *D* is the  $t = t_w$  signal. Peak *C* is for the background calibration purpose, and will be discussed later. The ratio of the total number of counts under peaks *D* and *B* gives the probability for the ion having decayed to the ground state after a time  $t_w$ .

It should be pointed out that, for a long-lived lifetime measurement, the off-state of the laser has to be nearly absolute. Even a very weak leakage of the laser power is

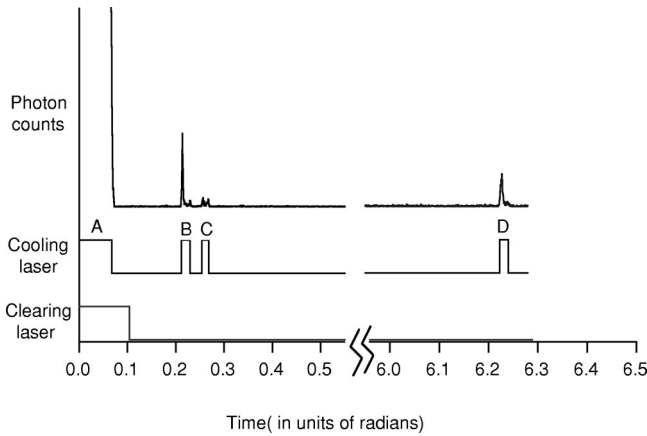


FIG. 3. The pulse sequence for the  $D_{3/2}$  state lifetime measurement. The time is indicated in radians. The actual time is obtained by multiplying  $1/(2\pi f_c)$ . The trace of photon counts in the plot was at  $f_c=9.3$  Hz.

enough to cause the allowed transitions to occur within the time scale of the measurement. Therefore, the laser pulses were generated using a custom-made mechanical chopper. Every revolution of the chopper completes one measurement cycle. For convenience, the wait time was varied by changing the chopping frequency  $f_c$ . Obviously, all pulse widths change with the chopping frequency. Accordingly, the horizontal time axis in Fig. 3 is indicated in radians. The corresponding times can be obtained by multiplying by the factor of  $1/(2\pi f_c)$ . The short uv pulses were generated by the holes of about 0.5-mm diameter at 42-mm radius, or 0.012 rad. The separation between the short uv pulses (the wait time) is about 6.1 rad. Therefore, the timing resolution is 0.2% regardless of the actual wait time. The fastest chopper speed used was 50 Hz, corresponding to about 20-ms wait time. The wait time  $t_w$  for data analysis was directly obtained from the number of bins in the MCS.

There are two background sources that must be removed from the peak signal counts. The first is the uniform room light background. It is independent of the chopper state, and can be readily subtracted. The second is the stray scattering of the uv laser, which is correlated with the chopping. To remove these scattered photon counts, an additional uv pulse (C in Fig. 3) was used immediately after the  $t=0$  uv pulse. Since the ion does not decay appreciably in this short time, the collected uv photons are the stray scattering, and therefore were subtracted from the peak signal after proper scaling of the pulse widths.

In the actual experiment, the wait time was varied from 20 to 160 ms. Figure 4 plots the decay probability vs the wait time. The error bars indicated are determined from the photon number statistics, i.e.,  $\delta n = \sqrt{n}$ . The timing errors are relatively small and not indicated in the figure. A weighted least-squares fit to the  $(1 - e^{-t/\tau})$  function gave  $52.7 \pm 2.4$  ms. The error is one standard deviation of the statistic uncertainty arising from the fit. The typical collisional quenching effect in single-ion measurements is on the order of  $10^7 s^{-1}$  per Torr [10,11], which is completely negligible in our measurement with  $10^{-10}$  Torr of background pressure. The 52.14

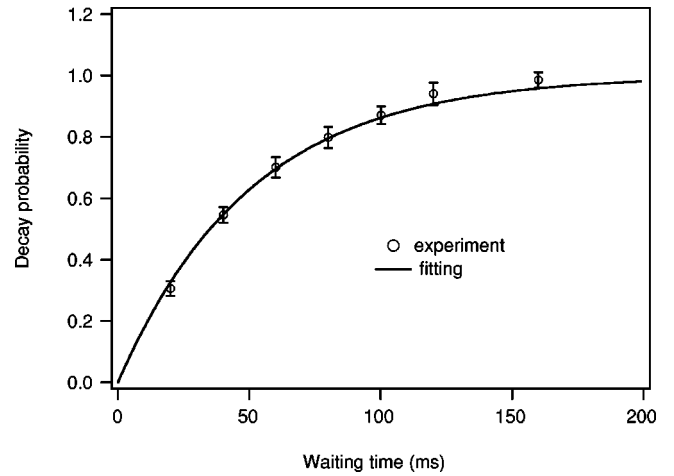


FIG. 4. The  $D_{3/2}$  state decay probability vs the wait time.

ms previously measured in buffer-gas-cooled clouds is consistent with the present single-ion result. The theoretical estimate of Fawcett and Wilson [14] is 41 ms, while that of Garstang [15] is 74 ms. It should be emphasized that the single-ion measurement here eliminated the need for an extrapolation of the pressure, and all known systematic errors are absent at the quoted uncertainty level.

As a by-product, the  $P_{1/2}$  branching ratio to the  $D_{3/2}$  state can be estimated from our measurement by counting the number of photons emitted during the  $t=0$  pulse before the ion ends in the  $D_{3/2}$  state. The overall photon-counting efficiency in our system was calibrated by saturating both the cooling and clearing transitions. At laser intensities ten times over the saturation intensities for both uv and red lasers, it is easy to show that the  $P_{1/2}$  steady-state population is 0.476. The detected resonant and heavily saturated fluorescence photon count was  $1.65 \times 10^4$ , i.e.,  $0.476 \eta \gamma_{ps} = 1.65 \times 10^4$ . With the  $P_{1/2}$  state decay rate  $\gamma_{ps} = 1.24 \times 10^8$  [16], the detection efficiency was found to be  $\eta = 2.80 \times 10^{-4}$ . Given the uncertainties in the degrees of saturation, we assign a 5% uncertainty in the detection efficiency estimate. The averaged photon counts per uv pulse was measured to be  $0.0580 \pm 0.0038$ . Note that this measurement is relatively robust since the average number of photons scattered per pulse is independent of the laser-induced transition rate and the pulse width. Thus one obtains the branching ratio to  $D_{3/2}$  to be 0.0483 with a 9% overall uncertainty, agreeing well with the theoretical calculation of 0.048 [17].

#### IV. MEASUREMENT OF $D_{5/2}$ LIFETIME

The  $D_{5/2}$  state is lying below the  $P_{1/2}$  states but is not connected to the laser-cooling transitions. It serves as the shelving state in the quantum jump experiment [18], and therefore the lifetime of this state can be conveniently determined with the quantum jump technique. In this technique, continuous fluorescence photons are detected when the ion is in the ground state. An excitation of the ion into the  $D_{5/2}$  state will quench the fluorescence completely, until it decays spontaneously back to the ground state and the fluorescence resumes. The on or off state of the fluorescence signal indi-

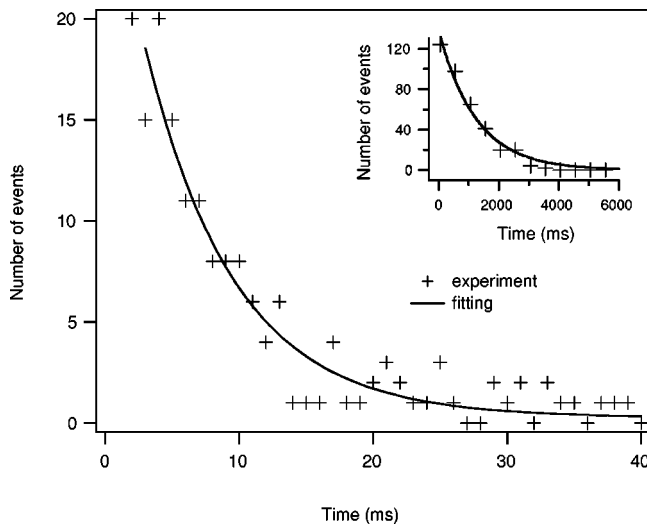


FIG. 5. The  $D_{5/2}$  state decay histogram with 1-ms bin width. The inset shows a similar plot for the ion out of the  $F_{7/2}$  state.

cates whether the ion is in the  $S_{1/2}$  or  $D_{5/2}$  state. The average fluorescence off-time (dark period) gives the lifetime of the  $D_{5/2}$  state. The ion excitation into the  $D_{5/2}$  state was achieved by exciting the  $P_{3/2}$  level. Instead of a 329-nm laser, we used a high-current Yb discharge lamp for this process. The lamp could make a shelving rate about  $0.3 \text{ s}^{-1}$ . However, the lamp increased the dark period counts to about 500 when used with a 329-nm interference filter.

There are two aspects which make the measurement in  $\text{Yb}^+$  more difficult than that in other alkalinelike ions. First, below the  $D_{5/2}$  state lies an additional  $F_{7/2}$  metastable state which is extremely long lived. Furthermore, the ion decays from the  $D_{5/2}$  state into the  $F$  state four times more often than back to the ground state [7]. Therefore, an additional clearing laser at 638 nm is necessary. Moreover, when the ion signal is off, the ion could either still be in  $D_{5/2}$  or have decayed to the  $F$  state. To exclude those events corresponding to decay

into the  $F$  state, the 638-nm clearing laser was adjusted so that the average dwell time in the  $F$  state was much longer than that in the  $D_{5/2}$  state. The second difficulty is that the  $D_{5/2}$  state lifetime is relatively short. One has to be able to determine the change of the state in a short (millisecond) time. We set our detection bin width at 1 ms, which still allowed reliable state detection.

Figure 5 shows the histogram plot of the ion signal dark periods. A weighted least-squares fit to an exponential decay  $e^{-t/\tau}$  yielded  $7.0 \pm 0.4$  ms. Again, the error is one standard deviation of the statistic uncertainty arising from the fit. The inset in the figure plots the same histogram on a much longer time scale. The “decay” rate of 1.3 s gives the average dwell time of the ion in the  $F$  state before it is pumped out by the 638-nm laser. Subtracting the long-time scale decay from the data and refitting the short-time decay resulted in no significant change in the  $D_{5/2}$  lifetime, as expected. This measured value agrees well with the previously measured value of 7.2 ms [7] within the quoted experimental error but significantly differs from a theoretical estimate of 5.7 ms [14].

## V. CONCLUSION

In conclusion, we have measured the natural radiative lifetimes of both  $4f^{14}5d$  states in  $\text{Yb}^+$  ion. The  $D_{3/2}$  measurement was carried out using single ions in the collision-free ultrahigh vacuum. The obtained values of  $52.7 \pm 2.4$  ms for  $D_{3/2}$  and  $7.0 \pm 0.4$  ms for  $D_{5/2}$  are consistent with the previous experimental values, but differ significantly from the theoretical calculations. The branching ratio of  $P_{1/2}$  into  $D_{3/2}$  was also measured to be 0.0483, with a 9% uncertainty. To our knowledge, this is the first experimental value for this parameter, and agrees well with the theoretical calculation.

## ACKNOWLEDGMENTS

This work was carried out at JPL under contracts from NASA. The authors thank Wei Wo for his contribution in the initial experimental setup.

- [1] R. Casdorff, V. Enders, R. Blatt, W. Neuhauser, and P.E. Toschek, *Ann. Phys. (N.Y.)* **48**, 41 (1991).
- [2] C. Tamm, D. Schnier, and A. Bauch, *Appl. Phys. B Lasers Opt.* **60**, 19 (1995).
- [3] P.T.H. Fisk, M.J. Sellars, M.A. Lawn, and C. Coles, *Appl. Phys. B Lasers Opt.* **60**, 519 (1995).
- [4] P. Gill, H.A. Klein, A.P. Levick, M. Roberts, W.R.C. Rowley, and P. Taylor, *Phys. Rev. A* **52**, R909 (1995).
- [5] M. Roberts, P. Taylor, G.P. Barwood, P. Gill, H.A. Klein, and W.R.C. Rowley, *Phys. Rev. Lett.* **78**, 1876 (1997).
- [6] P. Taylor, M. Roberts, G.P. Barwood, and P. Gill, *Opt. Lett.* **23**, 298 (1998).
- [7] P. Taylor, M. Roberts, S.V. GatevaKostova, R.B.M. Clarke, G.P. Barwood, W.R.C. Rowley, and P. Gill, *Phys. Rev. A* **56**, 2699 (1997).
- [8] G.R. Janik, Ph. D. thesis, University of Washington, Seattle, WA, 1984; I. Marzol, J.I. Cirac, R. Blatt, and P. Zoller, *Phys. Rev. A* **49**, 2771 (1994).
- [9] H.J. Kimble, *Cavity Quantum Electrodynamics* (Academic, New York, 1994), p. 203.
- [10] Ch. Gerz, J. Roths, F. Vedel, and G. Werth, *Z. Phys. D* **8**, 235 (1988).
- [11] N. Yu, W. Nagourney, and H. Dehmelt, *Phys. Rev. Lett.* **78**, 4898 (1997).
- [12] N. Yu, W. Nagourney, and H. Dehmelt, *J. Appl. Phys.* **69**, 3779 (1991); N. Yu and W. Nagourney, *ibid.* **77**, 3623 (1995).
- [13] N. Yu and H. Dehmelt, in *Trapped Charged Particles and Fundamental Physics*, edited by D.H.E. Dubin and D. Schneider (AIP, Woodbury, NY, 1998), p. 261.
- [14] B.C. Fawcett and M. Wilson, *At. Data Nucl. Data Tables* **47**, 241 (1991).
- [15] See Ref. 6 in Ref. [10].
- [16] E.H. Pinnington, G. Rieger, and J.A. Kernahan, *Phys. Rev. A* **56**, 2421 (1997).
- [17] J. Migdalek, *J. Phys. B* **13**, L169 (1980).
- [18] W. Nagourney, J. Sandberg, and H. Dehmelt, *Phys. Rev. Lett.* **56**, 2797 (1986).